Hindawi Publishing Corporation
Science and Technology of Nuclear Installations
Volume 2012, Article ID 158617, 17 pages
doi:10.1155/2012/158617

Research Article

Remarks on Consistent Development of Plant Nodalizations: An Example of Application to the ROSA Integral Test Facility

J. Freixa and A. Manera

Laboratory for Reactor Physics and Systems Behaviour (LRS), Paul Scherrer Institut (PSI), 5232 Villigen, Switzerland

Correspondence should be addressed to J. Freixa, jordi.freixa@psi.ch

Received 4 May 2011; Accepted 3 September 2011

Academic Editor: Klaus Umminger

Experimental results obtained at integral test facilities (ITFs) are used in the validation process of system codes for the transient analyses of light water reactors (LWRs). The expertise and guidelines derived from this work are later applied to transient analyses of nuclear power plants (NPPs). However, the boundary conditions at the NPPs will always differ from those at the ITF, and hence, the soundness of the ITF model needs to be maximized. An unaltered ITF nodalization should prove to be able to simulate as many tests as possible, before any conclusion is derived to NPP analyses. The STARS group at the Paul Scherrer Institut (PSI) actively participates in several international programs, where ITFs are being used (e.g., ROSA, PKL). Several tests carried out at the ROSA large-scale test facility operated by the Japan Atomic Energy Agency (JAEA) have been simulated in recent years by using the United States Nuclear Regulatory Commission (US-NRC) system code TRACE. In this paper, 5 different posttest analyses are presented, along with the evolution of the employed TRACE nodalization and the process followed to track the consistency of the nodalization modifications. The ROSA TRACE nodalization provided results in a reasonable agreement with all 5 experiments.

1. Introduction

In the last decades, integral test facilities (ITFs) have been used to validate thermal-hydraulic codes with the final objective of performing safety analyses for nuclear power plants (NPPs). The experiments carried out at facilities like PKL, LOFT, LOBI, BETHSY, or LSTF have been employed to build up expertise in the usage of system codes. User guidelines have been derived, models and correlations have been corrected or further developed, and limitations on the use of system codes have been identified. Such expertise is later on applied to the modelling of NPPs. One of the lessons learned with the use of ITFs for system codes validation is that even though a given code with a given nodalization is able to capture correctly the phenomena occurring in one test, it might not be the case in a successive test with different boundary conditions. This can be true even for single phenomena such as the critical flow at a break location, so that one should not assume that the phenomenon will be well simulated in an NPP model. As a matter of fact, it has to be considered that the conditions to be simulated in the NPPs differ from those simulated with the ITF models, so that confidence in the system code and the associated nodalization can be built only after successful simulations of a wide range of tests.

The large number of available experiments in test facilities like the ROSA large-scale test facility (LSTF) operated by the Japanese Atomic Energy Agency (JAEA) offers the possibility to validate various physical models under different conditions, at the same time developing guidelines and strategies for building up the system nodalization. When developing an ITF nodalization, it is essential to simulate as many tests as possible by using exactly the same nodalization. The extend of expertise and guidelines obtained by a model that is able to reproduce several tests at the same time is far larger than what one can obtain with few tests, because the performance of the models and correlations is tested in different conditions. Users must not resort to simulate the different tests independently, because if done so, the robustness and the soundness of the model will be lost. Generally speaking, each time a new test is simulated and modifications are introduced to the main model other than

initial or boundary conditions, all previous tests should be recalculated to assure the consistency of the modifications. In principle, any improvement undertaken in the nodalization must be valid for all previous tests. Obviously, this supposes a considerable effort, especially when various full models of facilities or power plants are to be maintained. Hence, it is recommendable to establish a clear and easy methodology, aimed at reducing the efforts of the analyst. Examples of this consistent quality assurance can be found in [1, 2].

The STARS group [3] of the Paul Scherrer Institut (PSI) actively participates in several international programs where ITFs are employed (e.g., ROSA, PKL). Several tests of the ROSA/LSTF have been simulated at PSI in the recent years, within the OECD/NEA ROSA 1 and 2 projects. These projects aim at addressing thermal-hydraulic safety issues relevant for light water reactors through experiments making use of the ROSA/LSTF facility. The experiments are used for the development and validation of simulation methodologies of the complex phenomena occurring during design basis accidents (DBAs) and beyond DBAs. ROSA/LSTF, operated by the Japan Atomic Energy Agency (JAEA), is a full-height and 1/48 volumetrically scaled test facility of a 1100 MWe-class pressurized water reactor (PWR). The facility allows to perform system integral experiments simulating the thermal-hydraulic responses at full-pressure conditions during small break loss-of-coolant accidents (LOCAs) and other transients. The reference plant is Unit-2 of Turuga NPP of the Japan Atomic Power Company.

A nodalization of the ROSA facility has been built in the PSI STARS group using the United States Nuclear Regulatory Commission (US-NRC) thermal-hydraulic code TRACE. The nodalization has been employed to calculate 5 different ROSA experiments, focusing mainly on small and intermediate break LOCAs. From test to test, sensitivity studies have been performed which have led to nodalization modifications and corrections. This paper focuses on the evolution of the nodalization, and the work carried out in order to maintain a sole nodalization able to satisfactorily simulate all the transients.

2. Model Description

The ROSA/LSTF nodalization has been produced by using the US-NRC thermal-hydraulic code TRACE (version 5.0). The nodalization had been derived combining the information of existing TRAC-p and RELAP input decks provided by JAEA together with the original technical drawings of the facility.

The TRACE model of the LSTF, shown in Figure 1, consists of a 3D vessel, two separate loops with two steam generators, and a pressurizer. The primary system is completed with pressurizer control systems (spray system, relief and safety valves, and base and proportional heaters) and safety injection systems (accumulators and low- and high-pressure injections). The secondary system is provided with main and auxiliary feedwater systems, a set of relief and safety valves, a main steam line, and a common steam header.

The 3D vessel component is composed by 20 axial levels, 4 radial rings, and 10 azimuthal sectors. The three first rings cover the core region, and the fourth ring represents the downcomer (DC). The heater rods are simulated by means of 30 heat structures, one for each section in the radial plane. The rods are grouped in three categories according to the power regions of the LSTF.

All bypasses are nodalized according to the geometrical specifications, and the friction k-factors were adjusted such that the mass flow at the bypasses during the steady-state calculation matched the experimental values. An additional leakage between the DC and the UP was added, as it was seen to be the only way to represent the evolution of the void fraction in the downcomer. The considerations that lead to the nodalization of this additional leakage will be discussed in Section 4.1.1.

The 8 control rod guide tubes (CRGTs) are simulated by 12 pipes connecting the core outlet with the upper head. The two inner CRGTs are linked geometrically with three different core volumes as shown in Figure 1. In order to keep the same connections from the core exit to the upper head (UH), the two inner CRGTs were split into three pipes. Volumes and sections were divided by three, while the hydraulic diameter was kept. Hence, each of the two inner tubes is simulated by means of three parallel pipes connected with three out of ten azimuthal cells of the inner ring. The other guide tubes are simulated by using a single pipe component for each tube.

The correct simulation of metal structures and heater rods is of main importance to capture the system behavior during small break LOCA (SBLOCA) and intermediate break LOCA (IBLOCA) scenarios. The ROSA nodalization developed at PSI includes all heat structures corresponding to walls, heated rods, unheated rods, internal metal structures, and support plates. All these components are simulated by a total of 53 heat structures.

The ROSA/LSTF has a core protection logic aimed at avoiding damage to the heater rods in the core, by limiting the maximum allowed core temperatures. Basically, the core power is decreased when the rods temperature rises above $\approx$960 K. The logic of this protection is included in the control system simulated within the TRACE input data set.

The two loops are simulated separately, and a single pipe component is used in the nodalization to represent the U-tube bundle. The pressurizer is nodalized with a 7-cell pipe. The steam generators are represented by separator components, and the heat losses through the outer walls are taken into account as well.

The countercurrent flow limitation (CCFL) model was activated in correspondence of two locations:

(i) the top plate at the top of the core region. The Wallis correlation [4] was used with the same coefficients specified in the OECD BEMUSE project ($m = 1.0$ and $c = 0.8625$) [5];

(ii) the steam generator (SG) inlet plenums and U-tube section. Again the Wallis correlation was used although in this case the coefficients suggested by Yonomoto [6] were used ($m = 1.0$, $c = 0.75$).

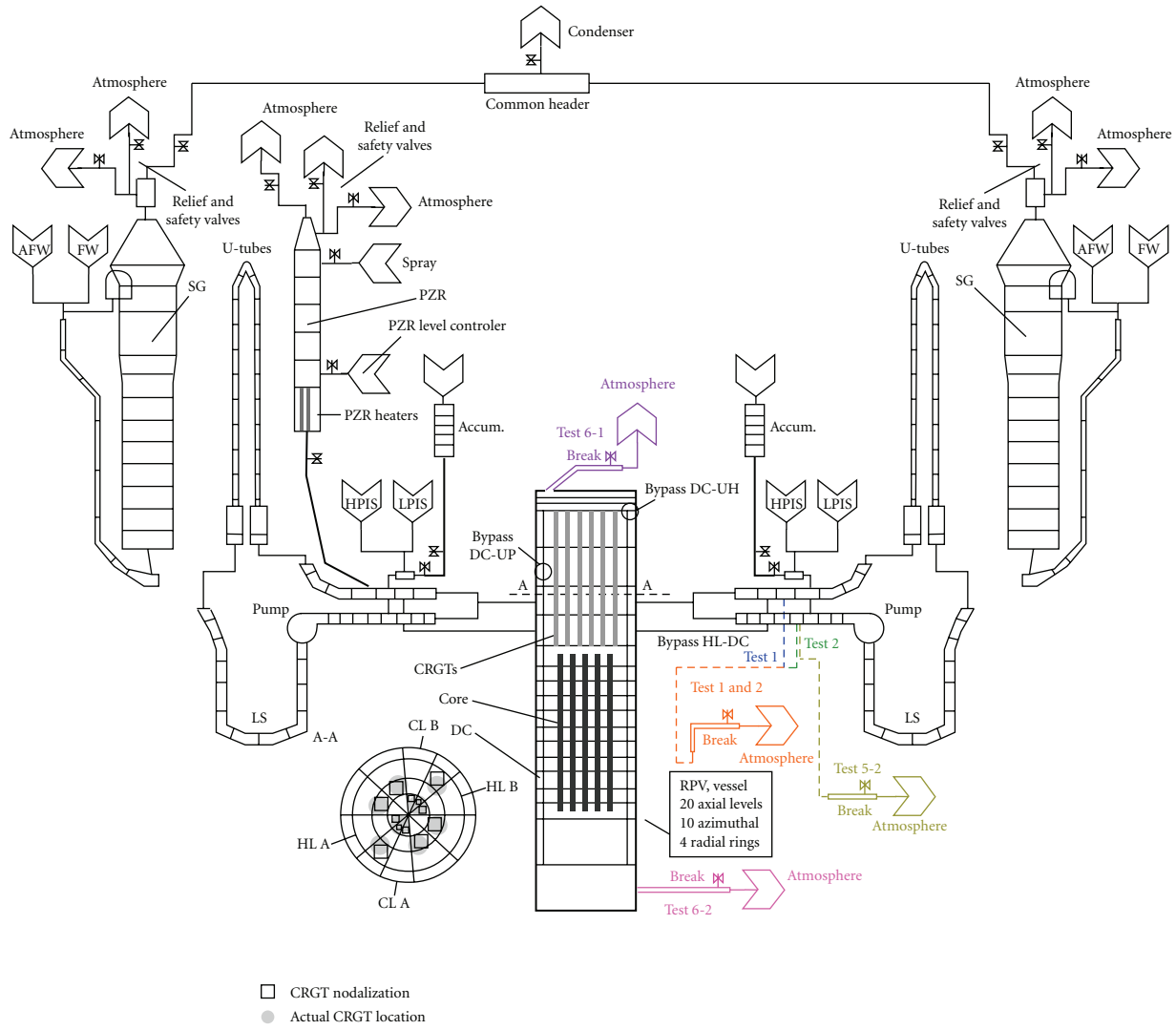

Figure 1: TRACE nodalization of the ROSA/LSTF.

2.1. Steady-State and Initial Conditions. A steady-state calculation was carried out in order to reach the experimental initial conditions. The initial conditions obtained by the TRACE model (Table 1) after the steady-state calculation are in quite close agreement with the experimental values. All steady-state parameters are within the error bands of the measurements. The most significant discrepancy is a 3% error in the steam flow rate. The high percentual errors in the bypasses flows are within the error bands of the measurements which are quite large.

The use of a three-dimensional vessel was seen to be crucial. Different flows were detected in the CRGTs depending on the position of the pipe relative to the vessel cross-section, that is, depending on the radial and azimuthal cell where the CRGTs were connected. While some CRGTs showed upward flow, others experienced downward flow, allowing natural convection in the upper head. Capturing this phenomenon was found to be crucial in order to correctly reproduce the UH temperature, which would have been otherwise too high.

Table 1: Percentual error between the calculated steady state and the experimental values.

	Percentual error (%)
Core power	0.0
DC to UH bypass flow	17.0
Hot leg to DC bypass flow	17.0
Primary pressure	0.3
Hot leg fluid temperature	0.3
Cold leg fluid temperature	0.2
Mass flow rate	0.0
Pressurizer level	2.0
Main steam pressure	0.0
Secondary side liquid level	0.5
Steam flow rate	1.9
Main feedwater flow rate	1.5

Table 2: Control logic of Test 6-1 [7].

Event	Condition
Break	Time zero
Generation of scram signal	Primary pressure 84% of initial value
PZR heater off	Generation of scram signal or PZR liquid level below 2.3 m
Initiation of core power decay curve simulation	
Initiation of primary coolant pump coastdown	
Turbine trip (closure of stop valve)	Generation of scram signal
Closure of main steam isolation valve	
Termination of main feedwater	
Opening and closing of the SG relief valves	SG pressures 110%/103%
Generation of SI signal	Primary pressure below 79% of initial value
Initiation of auxiliary feedwater	Generation of SI signal
Initiation of SG secondary-side depressurization as accident management (AM) action by fully opening relief valves	Core exit temperature reaches 623 K
Initiation of accumulator system	Primary pressure below 29% of initial value
Initiation of LPSI system	LP pressure below 8% of initial value

3. Tests

This section describes the final results of 5 different ROSA/LSTF tests that were simulated with the ROSA TRACE nodalization. The results shown in this section were obtained by the last integrated version of the model after simulating test 5-2 of the ROSA-1 project. All the relevant modifications undertaken during the process are described in Section 4. All tests start with the same initial conditions.

3.1. Test 6-1. Test 6-1 is an SBLOCA case with the break located in the UH of the reactor pressure vessel (RPV). The break was realized in the facility by using a sharp-edge orifice mounted downstream of a horizontal pipe that was connected to the upper head (the orifice flow area corresponded to 1.9% of the volumetrically scaled cross-sectional area of the reference PWR cold leg). The test started by opening the break valve, and by increasing at the same time the rotation speed of the primary coolant pumps up to 1500 rpm, for a better simulation of the expected pressure and flow values that would prevail in a similar transient in the reference PWR. Proportional heaters were used in the pressurizer (PZR) to control the primary pressure, while backup heaters compensated for system heat losses. The proportional heater power was turned off simultaneously with the activation of the scram signal, while the backup power was reduced and only completely shut down immediately after the PZR liquid level became lower than 2.3 m. This particular operation of the reactor coolant pumps and the PZR heaters was performed in all the tests analyzed in the work presented here. The description of the control logic of Test 6-1 is detailed in Table 2.

The scram signal was set to be dependent on the primary pressure by a set point of 84% of the initial pressure and initiated the core power decay, the primary coolant pumps coastdown, the termination of the feedwater system, and the closure of the main steam isolation valve. The safety injection (SI) signal was generated when the primary pressure fell below 79%. When the core exit temperature reached 623 K, depressurization of the steam generator secondary side as accident management action by fully opening the relief valves was initiated. The auxiliary feedwater was also triggered by the SI signal. The ECC system was directed towards the two cold legs and consisted of two accumulators (Accs) injecting at a primary pressure of 29% of the initial primary pressure and two low-pressure safety injection (LPSI) pumps that were started at a lower plenum (LP) pressure of 8%. The high-pressure safety injection (HPSI) system was not actuated in this test. Further details on the experimental procedures and results can be found in [7].

3.1.1. Results. Table 3 shows the chronology of the main events that occurred in Test 6-1, comparing the experimental values with the calculated ones. All the events in the TRACE simulation occur similarly as in the experiment. Discrepancies are found to be within a reasonable range of less than 80 seconds. The calculation was ended at 3000 seconds as all main events had occurred by that time.

The most important parameters for Test 6-1 are shown in Figure 2. Since the break was located at the top of the RPV, the transient can be easily divided into three different phases according to the break flow conditions: blowdown phase, break discharge in two-phase choked regime, and break discharge in single-phase vapor.

The first two phases, blowdown and two-phase flow phases, were simulated very well by the TRACE model. The distribution of coolant was correctly reproduced, as shown in the bottom graph of Figure 2. The early drop of the DC level and cold leg level (see [8]) (at about 250 s and 200 s, resp.,) could only be simulated assuming a hypothetical bypass between the UP and the DC (this assumption which will be explained and justified in Section 4.1.1). During this phase, the primary and secondary pressures were steady around the SG relief valves set points (middle graph of Figure 2). After

Table 3: Chronology of the main events in Test 6-1 [7].

Event	Exp.	TRACE
Break valve opened	0	0
Scram signal	26	20
SI signal	27	21
Break flow from subcooled to two-phase flow	50	46
Primary coolant pumps stopped	277	270
Break flow to single-phase vapor	700	741
Primary pressure lower than SG pressure, core level decreases	784	761
Full opening of SG relief valves	1090	1071
Core protection activated	1205	1271
Initiation of Acc system	1305	1225
Initiation of LPSI	2893	—
End of test	3266	3000

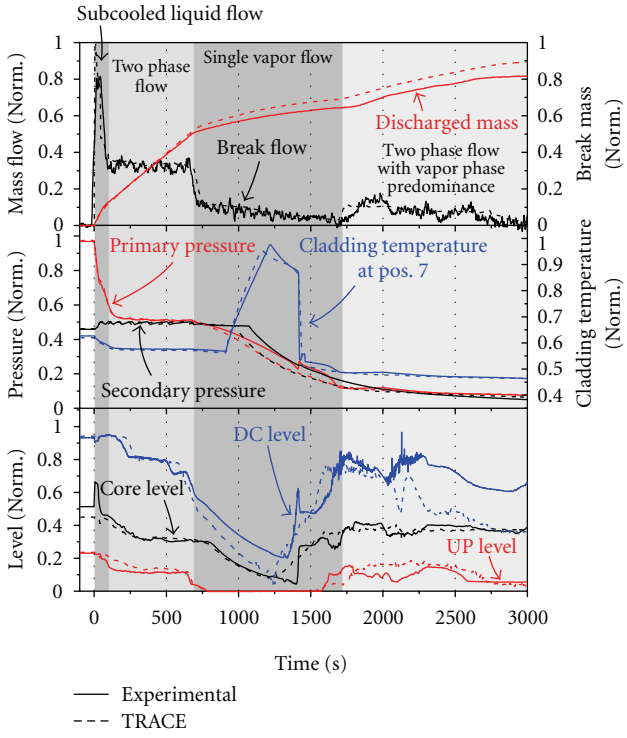

Figure 2: TRACE results for Test 6-1. From top to bottom: (1) break flow and integrated discharged mass, (2) primary and secondary pressure along with the maximum cladding temperature, and (3) RPV water levels.

this first reduction of mass inventory, the UP level dropped and the penetration holes at the bottom of the CRGTs started to void, and thus steam flew to the upper head and was expelled through the break. The transition from two-phase flow to single-vapor flow at the break was well matched by the TRACE nodalization although a delay in the transition of 50 seconds was detected. Due to this delay, the integrated discharged mass at the end of the two-phase flow part was higher in the simulation. Afterwards, the single-phase vapor choked flow at the break reported slightly higher values (see top graph in Figure 2). As a consequence, the primary pressure fell at a higher rate and the UH mass experienced a larger reduction. The drop of core level occurring during this phase was satisfactorily simulated (Figure 2). The maximum PCT, one of the most interesting signals of this test, was also correctly simulated by the model as shown in the middle graph of Figure 2. The PCT reached the core protection set points similarly in both the test and the calculation, and the power was reduced to 10% after the PCT reached 970 K. Afterwards, the PCT started to decrease. The core level started to rise again right after the opening of the accumulator valves (at $t = 1225$ s). Since the primary pressure decreased faster in the calculation, the valves opened earlier than in the experiment, so the core level rose earlier as well.

Further details on the simulation of Test 6-1 can be found in [8].

3.2. Test 6-2. Test 6-2 was started by opening a 0.1% break in the LP. The break was realized by using an inner-diameter sharp-edge orifice mounted downstream a horizontal pipe connected to the LP. The scram signal was triggered when the primary pressure was lower than 84% of the initial value [9]. The PZR heaters were operated as explained in Section 3.1 (page 4). The control logic of Test 6-2 is detailed in Table 4.

The SI signal was generated when the primary pressure decreased below 79%, and it was ensued by initiation of the auxiliary feedwater (AFW). Thirty minutes after the generation of the SI signal, asymmetrical steam generator secondary-side depressurization as accident management action was activated in order to achieve a depressurization rate of 55 K/h in the primary system. A loss of offsite power was considered, so that the HPSI pumps were not available. The LPSI and accumulator systems were fully operable and were actuated as shown in Table 4. Further details on the experimental procedures and results can be found in [9].

3.2.1. Results. Table 5 shows the chronology of the main events that occurred in Test 6-2, comparing the experimental values with the calculated ones.

The most relevant results of Test 6-2 are shown in Figure 3, which displays the cladding temperature, RPV collapsed water levels, primary and secondary pressures, and the loop mass flow rates. Overall good agreement between simulation and experimental results was obtained for the whole transient.

The primary and secondary pressures are shown in the third graph of Figure 3. During the first part of the transient, the primary pressure decreases slightly faster in the calculation, and therefore, some of the associated events occurred earlier (see the chronology, Table 5). Once the depressurization is started in loop B, the primary pressure remains close to the loop A secondary pressure until the reflux-condenser mode in this loop is interrupted (around 4000 s). Afterwards, the primary pressure follows the loop B depressurization. As shown in Figure 3, the primary pressure stabilizes around 15 bars during the latter period

Table 4: Control logic of Test 6-2 [9].

Event	Condition
Break	Time zero
Generation of scram signal	Primary pressure 84% of initial value
PZR heater off	Generation of scram signal or PZR liquid level below 2.3 m
Initiation of core power decay curve simulation	
Initiation of primary coolant pump coastdown	
Turbine trip (closure of stop valve)	Generation of scram signal
Closure of main steam isolation valve	
Termination of main feedwater	
Generation of SI signal	Primary pressure below 79% of initial value
Opening and closing of the SG relief valves	SG pressures 110%/103%
Initiation of auxiliary feedwater	Generation of SI signal
Initiation of asymmetrical SG secondary-side depressurization as AM action to achieve a depressurization rate of 55 K/h in the primary system	30 minutes after generation of SI signal
Initiation of accumulator system	Primary pressure below 29% of initial value
Initiation of LPSI	LP pressure below 8% of initial value

Table 5: Chronology of the main events in Test 6-2 [7].

Event	Exp.	TRACE
Break valve opened	0	0
Scram signal	569	453
SI signal	736	545
Primary coolant pumps stopped	819	708
Asymmetrical SG secondary-side depressurization	2548	2345
Closure of SG RV in loop with PZR	2679	2345
Initiation of accumulator system	≈5150	5450
Inflow of nitrogen gas from Acc, loop with PZR	≈10030	10995
Inflow of nitrogen gas from Acc, loop w/o PZR	≈11070	11013
Core uncovery	≈20400	22370
Initiation of LPSI	≈21940	—
Core protection activated	≈23270	23510
Second actuation of LPSI system	≈23320	—
End of transient	24034	24000

of the test (12000–25000 seconds), which overestimates the experimental results. On the one hand, the secondary-side depressurization stops at a slightly higher pressure. This depressurization depends on the capacity of the relief valve, and thus on its area and friction losses along the line. The k-factors along this line were adjusted according to the correct flows expected at high pressures. On the other hand, the higher pressure can also be caused by an overestimation of the injected nitrogen, or by an inaccurate treatment of the heat transfer in the U-tubes under the presence of nitrogen. The nitrogen concentrates in the U-tubes and induces a degradation of the heat transfer from the primary to the secondary system. As a consequence of having a slightly higher primary pressure, the set point for the LPSI intervention was never reached in the calculation, and hence, the core was not quenched as in the experimental test. In any case, it is important to notice that the set point in the facility was reached very late and with a very small margin (see small window in the third graph of Figure 3).

The evolution of the natural circulation in both loops is well predicted (bottom graph of Figure 3). After the primary pumps are completely stopped, the computed mass flows drop to the correct value. The end of natural circulation in loop A occurs slightly earlier in the simulation, and afterwards, the loop B mass flow was slightly overpredicted.

The maximum cladding temperature was measured in position 7 on rod (4,4) of element B17 (top graph of Figure 3). Two peaks were observed in the experiment, the first one was quenched by a temporary injection of the LPSI system, while the second peak reached the core protection set point, triggering a reduction of the core power. Afterwards, the LPSI system started again and quenched the core rapidly. In the calculation, the first peak did not appear, and the second one reached the first protection set point, and as the core power was reduced, the cladding temperature started to decrease slowly. However, quenching did not occur since the LPSI did not intervene in view of the too high primary pressure. Further calculations showed that the temperature would have kept rising when disabling the LSTF core protection system, leading eventually to core damage.

The DC, core, and upper plenum levels are displayed in the second graph of Figure 3. The overall behavior as simulated by means of the PSI TRACE nodalization is in accordance with the experiment. Reasonably, large discrepancies are observed when the LPSI system starts in the experiment and the primary system is refilled. There is also a time delay on the plunging of the core level at 2000 seconds.

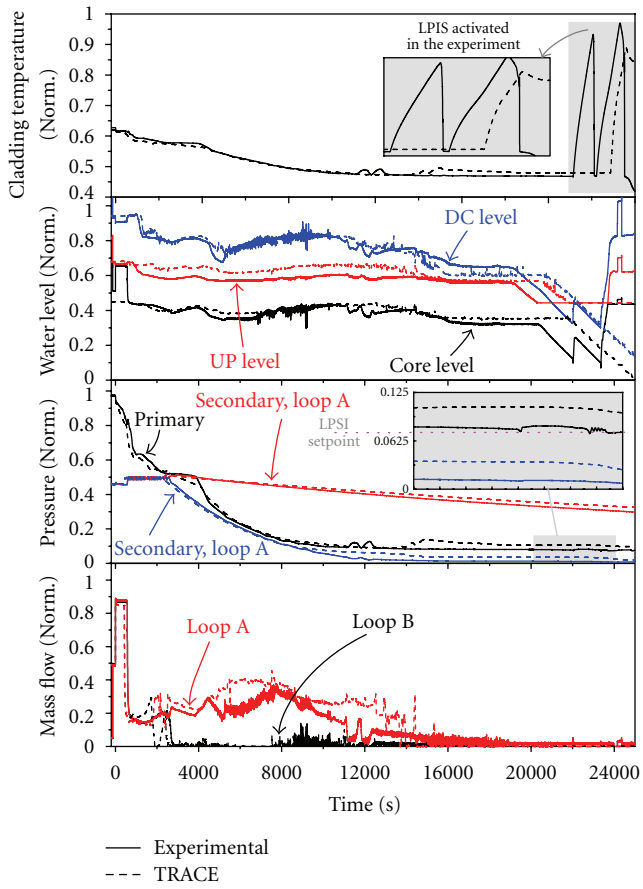

FIGURE 3: TRACE results for Test 6-2. From top to bottom: (1) cladding temperature in position 7 of rod (4,4), (2) RPV water levels, (3) primary and secondary pressures, and (4) loop mass flows.

3.3. Test 1. Test 1 is an intermediate break LOCA transient, in which a complete rupture of the surge line and the concurrent unavailability of the HPSI system are assumed. The control logic of the test is displayed in Table 6. The test is started by isolating the pressurizer and by opening the break valve located in the hot leg. Since a large amount of coolant is released through the break short after its opening, the primary pressure and the RPV level plunge. At the time when the hot leg of the broken loop becomes empty and the break flow switches from two-phase flow to single-phase vapor flow, the coolant that remains in the core starts to flash, and the core level is further reduced. An increase in the cladding temperature occurs as the heater rods become uncovered. Almost at the same time, the accumulator's valves open due to the drop of the primary pressure below the accumulators (Accs) set point. When the core level starts to drop, a large amount of steam is produced in the core, so that the pressure difference between the UP and the DC increases. The pressure drop is further enhanced by steam condensation in the cold legs due to the Acc's injection. When this pressure drop is large enough to drag the mass of water in the loop seal (LS), an LS clearance occurs. The core is refilled by means of the Acc's injection and the LS clearance. The timing between these three phenomena (Acc's injection, LS clearance, and break flow conditions) will confine the maximum peak cladding temperature.

The pressure set points for the opening and closure of the SG relief valves are 110% and 103%, respectively. Due to the assumed loss of offsite power, the HPSI is disabled for this test. The LPSI and Acc systems are available for this test and are actuated as shown in Table 6. Further details on this test and its simulation can be found in [10, 11].

3.3.1. Results. The chronology of the main events of Test 1 is shown in Table 7. All the events as simulated by TRACE occurred at very similar times as for the experiment (within 5 seconds difference), except for the initiation of the LPSI which was delayed in the experiment due to an increase of the primary pressure after the core was quenched. This increase in the primary pressure could not be explained by the experimentalists at the moment of writing.

The most important results of Test 1 are shown in Figure 4 where three different graphs display (from top to bottom): the break mass flow and integrated discharged mass, the primary and secondary pressures along with the PCT and the core, and UP and DC collapsed water levels.

The break flow in Test 1 was overpredicted by TRACE even though a two-phase discharge coefficient of 0.85 was used. The primary and secondary pressures were very well predicted once the discharge coefficient was reduced. The calculated maximum PCT was also found to be in accordance with the experimental results; however, the maximum PCT took place at a different elevation (around 1 meter difference). The maximum temperature in the TRACE calculation was detected at position 7 (see [12] for details), which is the place where the maximum PCT is usually detected. In the experiment, the maximum temperature was measured at position 5 instead (see [12] for details), which is about 1 meter below. This might be due to a slightly different core level evolution in the experiment. The water levels in the vessel are shown in the bottom graph of Figure 4 presenting a good agreement with the experiment.

3.4. Test 2. Test 2 is an intermediate break LOCA transient for which a complete rupture of the ECC line connected to the cold leg is assumed. The 17% break, corresponding to the volumetrically scaled cross-sectional area of the reference PWR cold leg, was realized by using a nozzle mounted on the top of the cold leg (upward direction). Due to the ECC line rupture, the ECC is only available in the intact loop. The failure of a diesel generator was assumed as well. Considering that the test intends to simulate a 4-loop Westinghouse design transient, the HPSI and LPSI flows injected into the intact loop correspond to 3/8 of the total nominal flow because, from the nominal 8 available pumps (2 per each cold leg), four are lost due to the failure of the diesel generator, and an extra one is lost because of the ECC line rupture. The Acc's volume to be injected in the intact loop corresponds to the volumetrically scaled volume of three Accs of the reference plant.

The control logic of the test is reported in Table 8. The test was started by opening the break; after the scram signal

Table 6: Control logic of Test 1 [10].

Event	Condition
Close of PZR spray line valves and PZR heaters	30 minutes before break
Isolation of PZR by closing surge line valve	1 minute before break
Break opening	Time zero
Generation of scram signal	4 seconds
Initiation of primary coolant pump coastdown	
Initiation of core power decay simulation	
Turbine trip (closure of stop valve)	Generation of scram signal
Closure of main steam isolation valve	
Termination of main feedwater	
Opening and closing of the SG relief valves	SG pressures 110% and 103%
Initiation of accumulator system	Primary pressure below 29% of initial value
Initiation of low-pressure injection system	LP pressure below 8% of initial value

Table 7: Chronology of the main events in Test 1 [10].

Event	Exp.	TRACE
PZR isolation	−60 s	−60 s
Onset of break	0 s	0 s
Scram signal	1 s	4 s
Turbine trip	1 s	4 s
Primary coolant pumps stopped	4 s	4 s
Main FW isolated	8 s	4 s
Start of decay heat	20 s	22 s
Actuation of ACC	154 s	155 s
PCT increases	164 s	163 s
Maximum PCT	182 s	185 s
Start of LPSI	504 s	349 s
End of test	1533 s	500 s

was reached, the typical sequence of action is realized: initiation of core power decay, initiation of primary coolant pumps coastdown, turbine trip, closure of main steam isolation valve, and termination of main feedwater flow.

Further details on this test can be found in [13].

3.4.1. Results. The chronology of the events taking place during Test 2 is shown in Table 9. Most of the events took place similarly in the simulation and in the experiment. The main difference is that in the simulation the core protection limit was not reached, and therefore the power was not reduced. As a consequence, the primary pressure remained slightly higher, and the LPSI setpoint was also not reached before the first 500 s of the transient. Some of the other discrepancies in the chronology are due to inconsistencies between the actuated experimental procedures and the ones described in the protocols since some experimental timings differ from the control logic shown in Table 8. For example, the initiation of the HPSI system was defined to be 12 seconds after the SI signal, but in the experiment, the HPSI started 25 seconds after the SI signal.

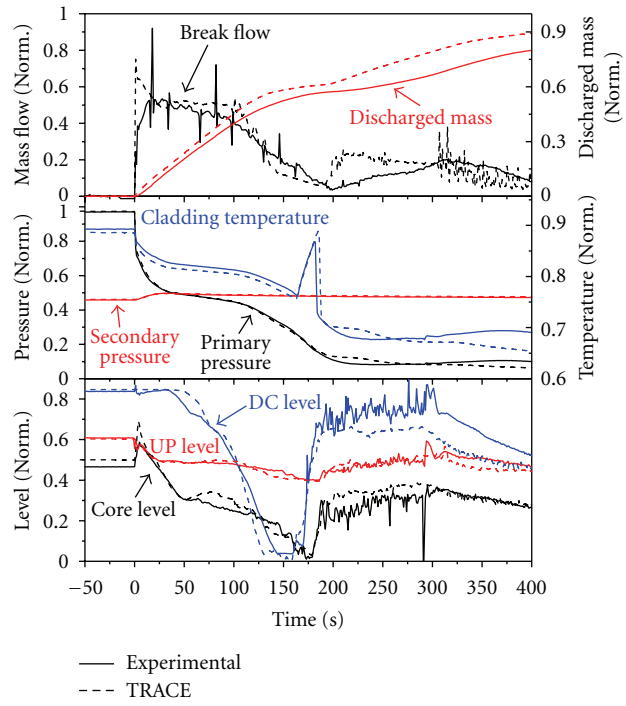

Figure 4: TRACE results for Test 1. From top to bottom: (1) break flow and integrated discharged mass, (2) primary and secondary pressure along with the maximum cladding temperature, and (3) RPV water levels.

The most relevant results of Test 2 are displayed in Figure 5: primary and secondary pressures, maximum PCT, break flow and integrated discharged mass, and the RPV collapsed water levels.

The top graph is showing the primary and secondary pressures along with the PCT at position 7. The primary and secondary pressures were found to be in good agreement with the experiment; however, the PCT was underestimated by about 20 degrees although the experimental temperature reached the LSTF protection system, and thus, the hypothetical maximum value that the PCT would have reached cannot

Table 8: Control logic of Test 2 [13].

Event	Condition
Break	Time zero
Generation of scram signal	Primary pressure 84% of initial value
PZR heater off	Generation of scram signal or PZR liquid level below 2.3 m
Initiation of core power decay curve simulation	
Initiation of primary coolant pump coastdown	
Turbine trip (closure of stop valve)	Generation of scram signal
Closure of main steam isolation valve	
Termination of main feedwater	
Generation of SI signal	Primary pressure below 79% of initial value
Initiation of HPIS in the loop with PZR only	12 s after SI signal
Initiation of accumulator system	Primary pressure below 29% of initial value
Initiation of low-pressure injection system	LP pressure below 8% of initial value
Opening and closing of the SG relief valves	SG pressures 110%/103%

Table 9: Chronology of the main events in Test 2 [13].

Event	Exp.	TRACE
Onset of break	0	0
Scram signal	5	6
SI signal	7	9
Turbine trip and MSIVs closed	10	9
Primary pumps trip	11	6
Termination of SG FW	13	6
SG relief valves open	≈27–57	≈25–55
Initiation of core power decay	29	24
Initiation of HPSI	≈35	21
Loop seal clearing	≈40	≈60
Primary pressure lower than SG pressure	≈55	74
Initiation of Acc system	≈110	126
Core protection activated	≈140	—
Max. PCT	≈150	141
Whole core was quenched	≈180	212
Primary coolant pumps stopped	260	256
Termination of Acc injection	≈280	≈285
Initiation of LPSI	≈290	—
End of test	1212	500

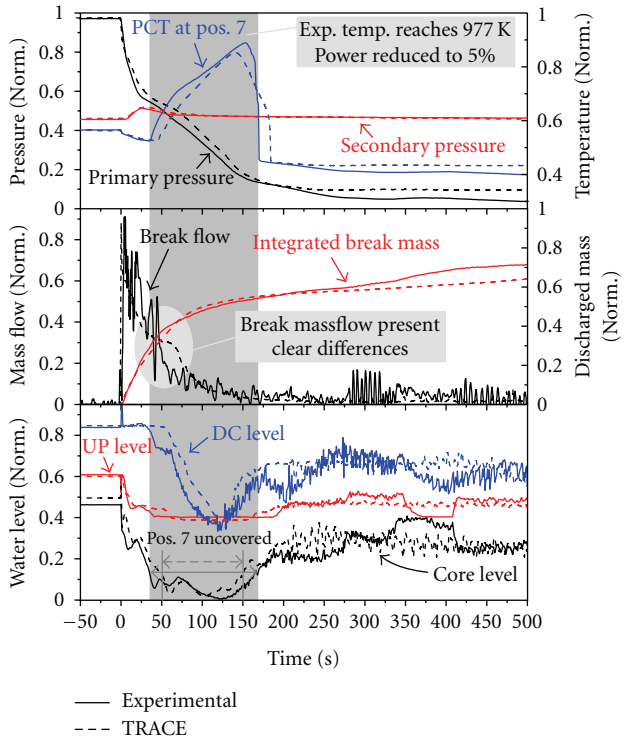

Figure 5: TRACE results for Test 2. From top to bottom: (1) primary and secondary pressure along with the cladding temperature at pos. 7 rod (4,4), (2) break flow and integrated discharged mass, and (3) RPV water levels.

be known. In this sense, it is better to examine the core water level shown in the bottom graph of Figure 5. Overall, the water levels in the RPV were well predicted by TRACE. However, as indicated in Figure 5 the window of time where the heated rods were uncovered was slightly longer in the experiment, and therefore, the PCT was underpredicted. The graph in the middle focus on the break mass flow and the integrated discharged mass. The time evolution of the break flow was not correctly simulated by TRACE. Even though the break device was identical to the one used in Test 1, in this case, the break mass flow under subcooled conditions was underpredicted (first 30 seconds, see Figure 16 for details). Figure 5 shows results with a two-phase choked coefficient of 1.1. It was found that the variations on the subcooled choked coefficients had no effect on the results, probably due to a limitation of the flow within the TRACE code (which could be derived from an internal bug), and the two-phase choked coefficient was increased to compensate the total discharged mass rather than to better predict the flow during this phase. Even though small modifications of the discharge coefficients are in general accepted by the international community, these changes must be consistent, and the user must not use

Table 10: Control logic of Test 5-2 [14].

Event	Condition
Break	Time zero
Generation of scram signal	Primary pressure 84% of initial value
PZR heater off	Generation of scram signal or PZR liquid level below 2.3 m
Initiation of core power decay curve simulation	
Initiation of primary coolant pump coastdown	
Turbine trip (closure of stop valve)	Generation of scram signal
Closure of main steam isolation valve	
Termination of main feedwater	
Generation of SI signal	Primary pressure below 79% of initial value
Opening and closing of the SG relief valves	SG pressures 110%/103%
Initiation of SG secondary-side depressurization by fully opening of the relief valves with auxiliary feedwater	10 minutes after generation of SI signal
Initiation of enhanced SG secondary-side depressurization by fully opening of safety valves	Primary pressure below 13% of initial value
Initiation of accumulator system	Primary pressure below 29% of initial value

different values depending on the case (unless the break conditions and geometry are very different). The differences observed between Tests 1 and 2 indicate that a revision of the choked flow of the TRACE code is needed. As a matter of fact, the choked flow in the latest version of TRACE (TRACE 5.0 patch 2) has been improved, and the problems experienced in Test 2 might have been solved, nonetheless additional problems may arise with the new code version (see Section 5 on page 15 for further details on this issue).

3.5. Test 5-2. Test 5-2 is a small break LOCA located in the cold leg of the loop without PZR. The test was started by opening a 0.5% break which was realized in the facility by using an inner-diameter sharp-edge orifice. The boundary conditions and control logic of this test is shown in Table 10. As for previous tests, the scram signal was actuated when the primary pressure fell below 84% of the nominal value and triggered the typical events for an SBLOCA case, as described in Table 10.

The SI signal was generated when the primary pressure decreased below 79%. Ten minutes after the generation of the SI signal, full symmetrical SG secondary-side depressurization as accident management action was activated by fully opening the relief valves. Auxiliary feedwater was also activated concurrently. When the primary pressure fell below 13%, enhanced SG secondary-system depressurization was started by fully opening the safety valves.

A total failure of the HPSI system was assumed in the test. The accumulators started to discharge when the primary pressure was reduced below 29%. The LPSI was disabled for this test, in order to observe the phenomena occurring in the SG under the influences of gas inflow when the primary pressure is below the LPSI actuation pressure. The logic of the ROSA/LSTF core protection system for Test 5-2 was the same as the one used for Test 6-1. Further details on this test can be found in [14].

Table 11: Chronology of the main events in Test 5-2 [14].

Event	Exp. (s)	TRACE (s)
Break valve opened	0	0
Scram signal	95	65
SI signal	145	112
Primary coolant pumps stopped	349	319
full opening of SG relief valves	756	696
AFW starts	756	696
Initiation of Acc system	≈1320	1293
Full opening of SG safety valves	≈2420	2586
End of test	13376	12000

3.5.1. Results. The chronology of the main events of Test 5-2 are shown in Table 11, where the experimental results are compared with the calculation. Due to a slightly overprediction of the depressurization rate of the primary side at the beginning of the transient, all the events in the simulation occurred about 30 seconds earlier than in the experiment.

The most relevant results obtained for Test 5-2 are displayed in Figure 6 (break flow and discharged mass, primary and secondary pressures, and RPV collapsed water levels).

The simulation of Test 5-2 is in fair agreement with the experiment. The primary and secondary pressure trends were correctly simulated by the ROSA TRACE nodalization. In Figure 6, the first 1000 seconds are zoomed in for a better view on the comparison between experiment and calculation. In a similar manner as in Test 6-2, the depressurization rate at the beginning of the transient was slightly overpredicted by TRACE. The full depressurization of the system by opening the relief valves and later on the safety valves was steeper at the beginning and slower at the end although the overall evolution in the simulation is acceptable. The initial break flow (first 1000 s of transient) was correctly

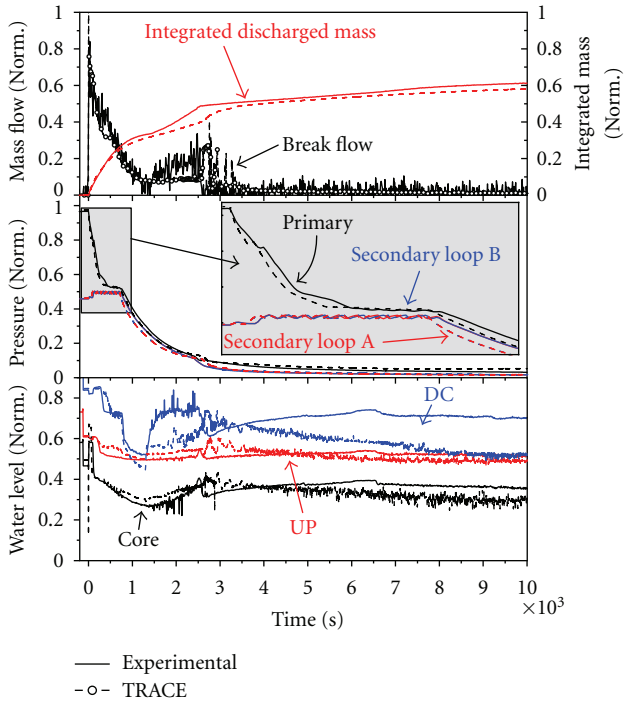

Figure 6: TRACE results for Test 5-2. From top to bottom: (1) break flow and integrated discharged mass, (2) primary and secondary pressures, and (3) RPV collapsed water levels.

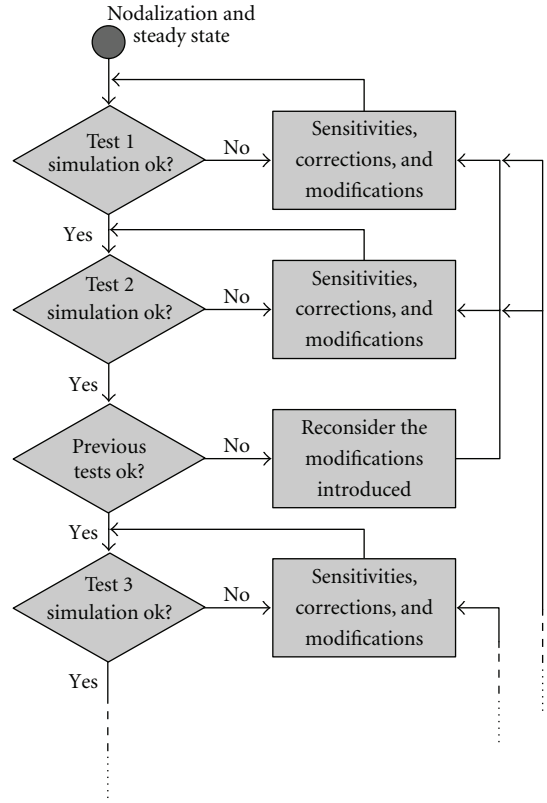

Figure 7: Flowchart for the model maintenance.

reproduced. Afterwards, discrepancies on the DC level were observed, as well as for the break flow (from 1000 to 3000 seconds).

All in all, a good agreement with the experimental results was obtained.

4. Model Evolution

The results presented in Section 3 were all obtained with the same TRACE nodalization, and only the boundary conditions specific for each test were modified from case to case. However, when the tests were first simulated, modifications and corrections of the nodalization accompanied by sensitivity studies were needed. The control systems were finally modified with the aim of allowing the user to run all previous cases with a minimum number of changes. In order to ensure the consistency of the modifications introduced, all previous tests were recomputed with the updated model after each posttest. To perform this action, it is important to maintain the model as compact as possible and to keep track of the included modifications. A basic methodology has been drawn for this purpose, which allows the user to recalculate any previous transient at any time in order to assure any important modification. The flowchart followed for the maintenance of the TRACE input deck is shown in Figure 7.

Basically, once the nodalization is developed and a satisfactory steady state is achieved, the nodalization is applied to the simulation of a first experimental test. At this stage, the original nodalization might be modified on the basis of sensitivity tests, in the case that the comparison with the experimental data is not satisfactory and the deficiencies are identified to be in the nodalization approach and not in the constitutive correlations hardwired in the system code. Then, the same nodalization is used to simulate a second test. Again, changes to the nodalization might be necessary to correctly reproduce the significant phenomena of the given experimental test. This time, however, before proceeding to the simulation of a third test, the nodalization would be applied "as it is" to the simulation of the previous test, in order to ensure that the modifications to the nodalization do not lead to unsatisfactory behaviors (i.e., the results obtained with the new nodalization should remain in close agreement with the previous validation results or result in an even better agreement with the experimental data). Once this step is concluded satisfactorily, the analyst can proceed to a third test, and so on. A compromise might be required between two different nodalizations when the results of previous tests are worsened. In this case, one nodalization must be picked up as the most appropriate.

This very procedure was employed at PSI for the TRACE ROSA nodalization presented in this work.

The ROSA/LSTF TRACE nodalization developed at PSI has been used for more than 5 years and has therefore undergone several modifications. The most relevant of those are described in the following chapters. Since the modifications and corrections to the nodalization were triggered by the discrepancies found when comparing to a given experimental test, they are classified accordingly.

4.1. Corrections Introduced during the Simulation of Test 6-1

4.1.1. Leakage from the Upper Plenum to the Downcomer. The cold leg and DC level evolution during the first part of Test 6-1 (until 700 s) pointed out interesting differences between the TRACE model and the experiment. While the level evolution in the core, upper plenum, upper head, and hot legs were reasonably predicted, the cold leg and DC level could not be correctly simulated. What the TRACE nodalization was not able to simulate was exactly the DC pressure drop, which was reduced in the experiment after the interruption of the natural circulation. The root of the discrepancy was the earlier presence of steam in the upper part of the DC, which modified the pressure drop inducing an earlier drop of the DC and the cold leg water levels. A series of sensitivity calculations was performed to analyse the possible reasons. After investigating all plausible causes and following the recommendations given in [15], it was concluded that the discrepancy could derive from a hypothetical leak from the DC to the upper plenum through the seal of the core support barrel. This seal ring was broken in August 1995, when the UH-UP bypass was plugged and then repaired in November 2001. It was found out that both the cold leg and the DC level evolutions were correctly simulated if a small leakage (1% of steady-state core flow) was assumed to exist in this region. The results of the DC and cold leg levels with and without the leakage are shown in Figure 8. Further details on this analysis can be found in [16]. This modification was then kept for the simulation of all successive tests producing a closer or equal agreement for all tests.

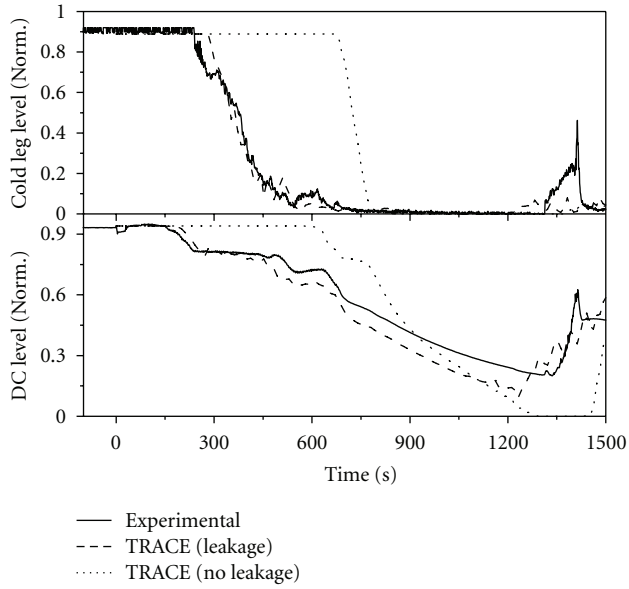

Figure 8: Collapsed water levels of the DC and the cold leg for Test 6-1 with and without a leakage between the UP and the DC.

4.1.2. UH Nodalization. Test 6-1 constituted a perfect experiment to study the performance of the choked flow model, since the location at the top of the RPV allowed a clear differentiation between the phases that a choked flow may experience, namely, subcooled-liquid phase, two-phase, and single-phase vapor flows (Figure 2 on page 5). The TRACE nodalization performed very well for the first two phases; however, when the flow at the break turned into single-phase vapor, the break flow rate was overestimated by TRACE. Sensitivities on the break nodalization and possible modifications on the TRACE model were carried out and constituted the bulk of a previous publication [8]. One of the main modifications to the model consisted in a refinement of the nodalization of the RPV upper head. As a matter of fact, it was found that a finer nodalization of the upper head was essential to correctly predict the void fraction and the saturation temperature at the break location. Initially, only one axial level between the CRGTs exits and the top of the RPV (0.504 m of height) was used. In order to enhance mixing and allow convection in this region, the number of axial levels was finally increased. With this modification, the steam temperature at the break inlet was more accurately predicted (around 2 degrees lower). It is important to notice that the gas velocity under single-phase vapor conditions and choked flow is basically a function of the stagnant temperature and the specific heat ratio; hence, an accurate prediction of the temperature close to the break is crucial. In this simulation, with an increased number of cells, the saturation temperature at the break was reduced and so was the break mass flow (see Figure 9 for details). The initial nodalization with only one axial level was split in three and 6 smaller nodes of 0.168 m and 0.084 m of height, respectively. There was almost no difference between the results obtained with 3 and 6 additional levels, but the computational time was very high for the 6-level calculation. Therefore, 3 levels for the upper part of the UH were used in the final nodalization (i.e., 20 axial levels for the entire RPV). The improvement obtained in the simulation of the break mass flow can be seen with the integrated break flow plotted in Figure 9. Further details can be found in [8].

4.2. Corrections Introduced during the Simulation of Test 6-2.

After a satisfactory simulation of Test 6-1, the same TRACE nodalization was employed for the simulation of Test 6-2. As a first approach, an early interruption of natural circulation was predicted leading to an increase of the primary pressure, as shown in Figure 10. Afterwards, the transient evolution could not be correctly captured by the simulation. The early stop of natural circulation (NC) indicated a wrong estimation of the U-tube levels and heat transfer to the secondary side. The reason could be related to the use of a single U-tube in representation of the whole bundle. However, it was found eventually that the U-tube nodalization (1 pipe) was too coarse and the discrepancies could be fixed by simply refining the axial nodalization of the corresponding pipe component. Figures 10 and 11 show the pressure and the mass flow in loop B, respectively, obtained with the two nodalizations. The old and new nodalization of the SG are shown in Figure 12.

The new nodalization was then used to simulate again Test 6-1. The results were improved with the new nodalization.

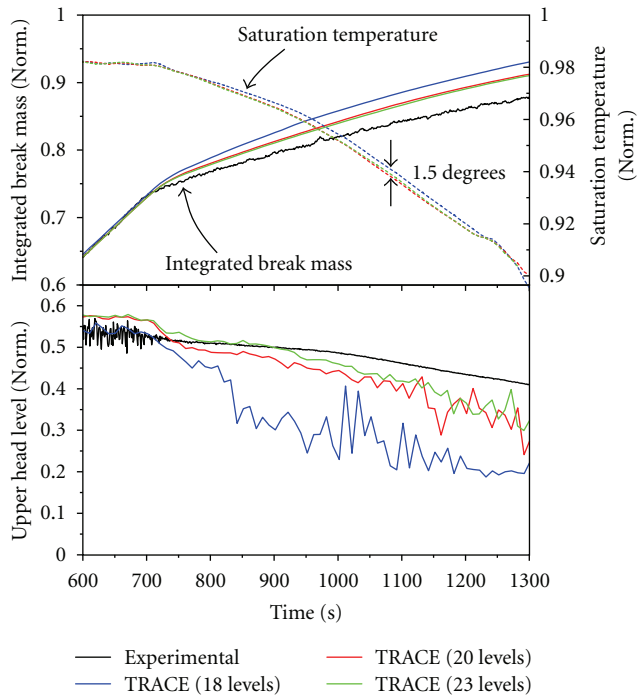

FIGURE 9: Sensitivity on the UH nodalization for Test 6-1 with finer and coarser meshing of the UH. Top: integrated break mass and saturation temperature at the top of the UH dome. Bottom: UH collapsed water level.

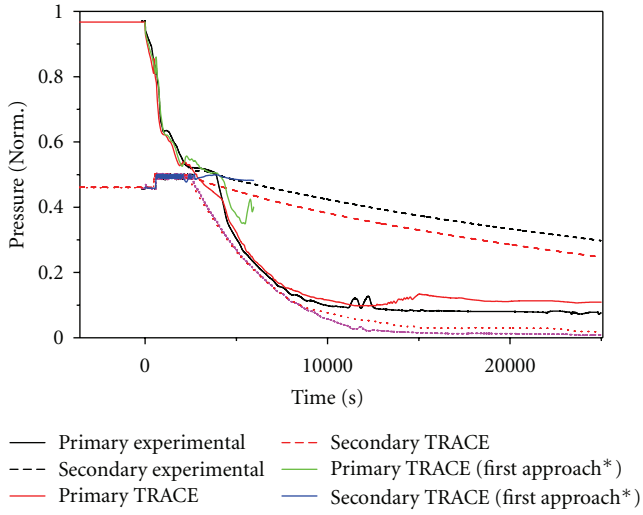

FIGURE 10: Primary and secondary pressures for Test 6-2 using both nodalizations of the SG's primary and secondary sides.

4.3. Corrections Introduced during the Simulation of Test 1. Test 1 was first carried out as a blind calculation along with the evaluation of its uncertainties [11], performed by applying the GRS SUSA methodology [17, 18]. Even though the maximum PCT temperature in the blind calculation showed lower values than in the experiment, the accompanying uncertainty evaluation helped confining the possible problems. Three modifications were included in the nodalization

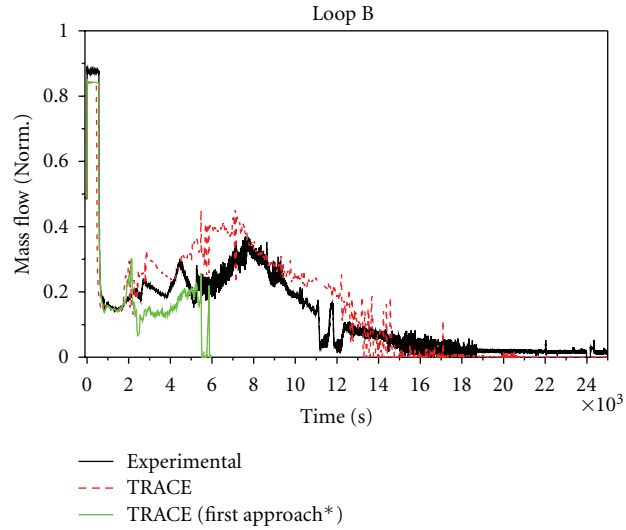

FIGURE 11: Mass flow in loop B using both nodalizations of the SG's primary and secondary sides.

used for the posttest calculation: a correction of the Acc's lines, the reduction of the two-phase choked coefficient, and the inclusion of the CCFL model at the top of the core.

The blind calculation of Test 1 displayed considerably larger accumulator flows than the experiment; hence, this line was revised and finally renodalized from scratch, in order to achieve a better representation of the pressure drops along the line. Figure 13 shows the results of the blind calculation and the modification on the Acc's line. It must be noticed that the rest of modifications included during the posttest process further increased the quality of the Acc's mass flow results (line labeled as "final TRACE result" in Figure 13).

Since the break flow was clearly overestimated during the two-phase flow regime, a parametric study on the two-phase choked flow coefficient was performed. A coefficient of 0.8 provided results in a closer agreement with the experiment, as shown in Figure 14. The final coefficient used for this test was 0.85. This modification was introduced after recalculating the test by following the methodology for a consistent nodalization.

The height of the PCT was confined by two factors. On the one hand, the time difference between the start of the core uncovery and the LS clearance was crucial for this transient. Both the LS clearance and the Acc's injection helped quenching the core. However, it was the LS clearance the phenomenon that triggered the reflood of the core. LS clearance occurs when the pressure difference between the UP and the DC is large enough to drive the LS water column into the DC. This occurred thanks to steam condensation in the cold leg with the injection of cold water from the Accs. The second phenomena that will define the height of the maximum PCT is the speed at which the core level drops during this window of time. The first phenomenon here described was well simulated even in the blind calculation; however, the level decreased at a slower rate, and therefore, the PCT was lower.

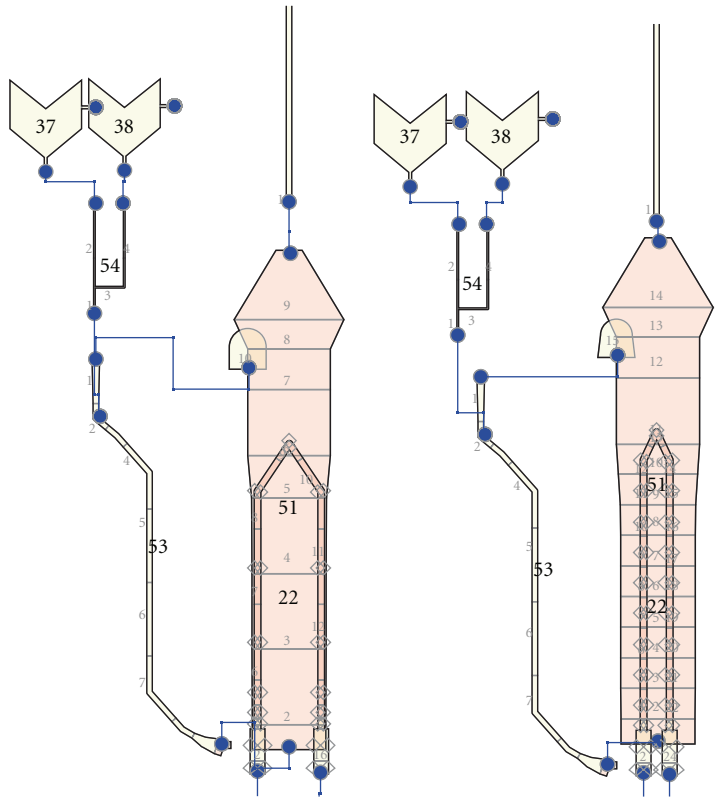

Figure 12: Old and new nodalization of the SG and U-tubes. Modification introduced during the analysis of Test 6-2.

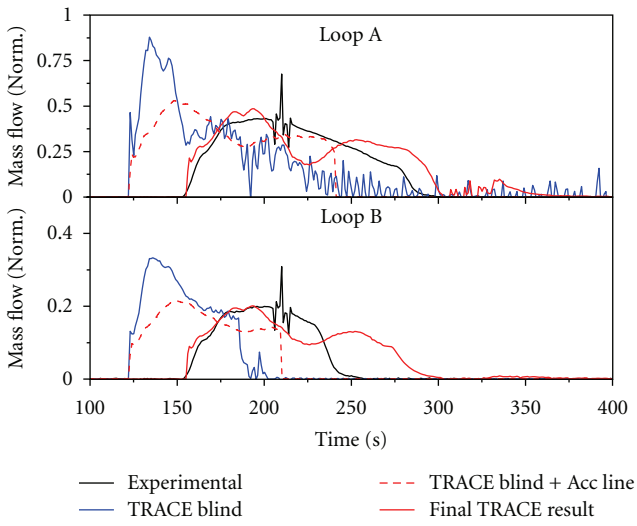

Figure 13: Accumulator injection during Test 1 with the new nodalization of the Acc's lines.

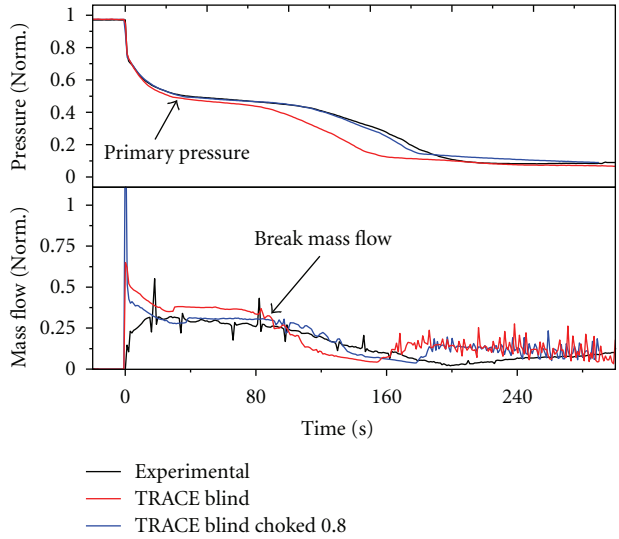

Figure 14: Primary pressure and break mass flow for Test 1, pretest results with different two-phase break discharge coefficients.

At this point of the analysis, it became obvious that an additional phenomenon significant for the evolution of this transient was the occurrence of CCFL conditions at the top of the core. Due to the fact that the CCFL was (mistakenly) not activated for the blind calculation, the core level remained higher than in the experiment due to the amount of water falling from the UP. In the experiment, the drop of water falling from the UP was prevented by the steam flowing out of the core. Once the CCFL model at the location of the upper core plate was activated, the core level dropped faster, in better agreement with the experimental data. The effect of using the CCFL model is shown in Figure 15, where the results of the cladding temperature are shown for

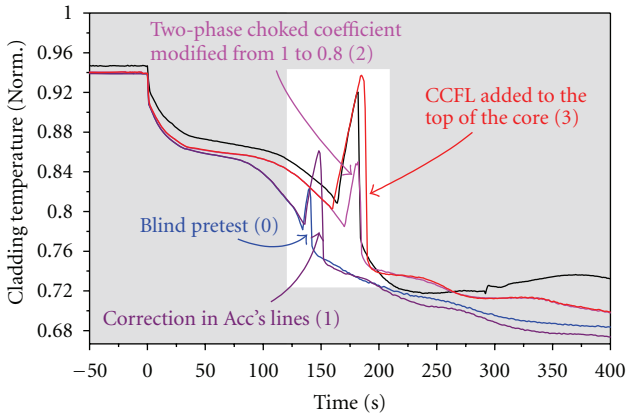

Figure 15: Maximum PCT for Test 1, evolution of the results with different modifications.

the different posttest steps. Summarizing, starting from the blind calculation, firstly the accumulator's lines were corrected, then the two-phase choked coefficient was decreased, and finally the CCFL model was used at the top of the core. Further details on these modifications can be found in [11].

After this nodalization modifications, all previous tests were recalculated, and there was no significant difference.

4.4. Corrections Introduced during the Simulation of Test 2. Since the IBLOCA of Test 2 occurs in the cold leg, CCFL phenomena may take place at the entrance of the U-tubes or at the connection between the pipes and the SG plenums. Therefore, the CCFL was activated in this region during the simulation of Test 2, and the simulation results were consequently improved. All cases were recalculated satisfactorily. For Test 1, the choked two-phase flow coefficient was slightly shifted from 0.8 to 0.85.

4.5. Corrections Introduced during the Simulation of Test 5-2. For this test, only corrections on the control systems in order to accommodate the test particularities were introduced. No further modification to the nodalization was necessary. However, all previous tests were recalculated to avoid any inconsistency or possible error introduced during the configuration process.

5. Choked Flow Response

The modeling of choked flows is one of the most important issues in nuclear thermal hydraulics, since it affects the prediction of the flow-rate at break locations, and therefore plays a key role in the evolution of all LOCA transients. The tests performed in LSTF within the ROSA-1 and 2 projects dealt with breaks of different sizes and location and thus provided a good database to evaluate the performance of the TRACE chocked flow models.

The v5.0 version of the TRACE code has been used for all simulations presented in this paper and has provided a good agreement with the experiments. The discharge coefficients used for each test are described in Table 12.

Table 12: Choked flow discharge coefficients used for all break locations, subcooled discharge (C_{sub}) and two-phase flow discharge (C_{2p}) coefficients.

Test	Type	C_{sub}	C_{2p}
Test 6-1	Orifice	1.0	1.0
Test 6-2	Orifice	1.0	1.0
Test 1	Nozzle	1.0	0.85
Test 2	Nozzle	1.0	1.1
Test 5-2	Orifice	1.0	1.0

A coefficient of 1.0 was used in all the orifice breaks providing reasonable enough results. However, for the two nozzle cases, the use of different two-phase flow discharge coefficients (C_{2p}) was needed even though they presented exactly the same geometry.

The disagreement of the choked flow patterns obtained for Test 2 and especially the need to use different discharge coefficients than those used for Test 1 motivated us to test newer versions of the code. Even though small modifications on discharge coefficients are in general accepted by the international community, these must be consistent, and the user must not use different values depending on the case (unless the break conditions and geometry are very different). The differences observed between Tests 1 and 2 indicated that a revision of the choked flow of TRACE was required. Once we tested the same model with the latest official release of the code (TRACE 5.0 patch 2), it was found out that the choked model was providing indeed a much better agreement with the experiment. Further studies indicated that, in Test 2 by using v5.0, the subcooled choked flow (first 33 seconds) was limited within the code subroutines, so that variations of the subcooled discharge coefficient (C_{sub}) would not have an impact on the results. As a matter of fact, a sensitivity on the C_{sub} showed that the results were influenced only when values of C_{sub} under 0.85 were being employed, so all calculations with a higher coefficient were equivalent with those obtained with a coefficient of 0.85 (see Figure 16). This behaviour was not observed by using the latest TRACE release. Since the flow was much lower at the beginning of the transient (with the v5.0 RC3 version), a higher value for the C_{2p} was needed to compensate the total discharged mass (see Table 12). This explains the differences between the C_{2p} used in Tests 1 and 2. It is important to point out that the subcooled break flow in the rest of the tests does not play an important role, and this might be the reason why this problem did not become evident until the simulation of Test 2.

The problems with the subcooled part of the choked flow model have been solved in patch 2; however, other issues have arisen with this version which hinders its usage. The methodology presented in this paper can also be used to quickly test new code versions, and in this case, patch 2 presented several deficiencies indicating that the new version cannot be used consistently.

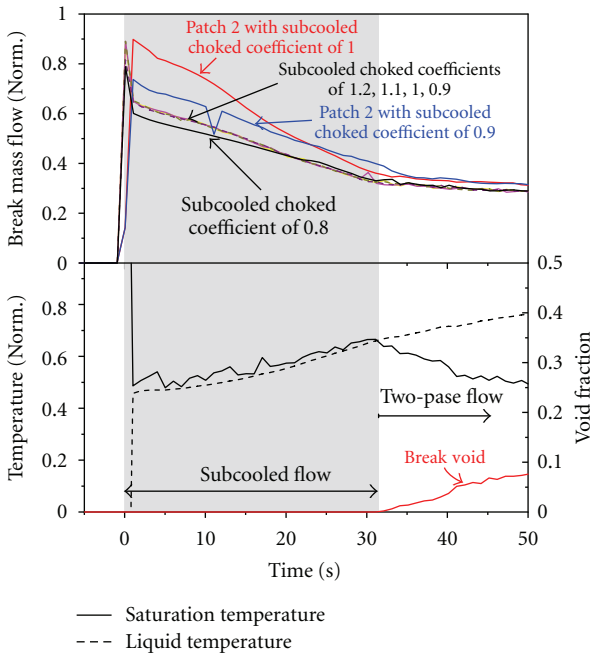

FIGURE 16: Break mass flow during the subcooled phase for Test 2; different subcooled choked coefficients are used for the TRACE v5.0 RC3 and patch 2 versions.

6. Conclusions

A nodalization of the ROSA/LSTF facility has been developed by using the US-NRC system code TRACE v5.0. The nodalization has been used to simulate 5 different tests focused on small and intermediate break LOCA cases. The simulations have been performed during the last 4 years; however, the model evolution has been tracked, and a methodology has been drawn to maintain a single consistent nodalization for all tests. Every time that a new posttest analysis was completed, the previous posttests simulations were carried out again, in order to guarantee that any new modification to the nodalization would only improve the overall performance of the nodalization. Finally, a reasonable agreement with all of the five tests was obtained. However, the calculated subcooled choked flow in Test 2 underestimated the experimental results. It was found out that the subcooled choked flow in the TRACE v5.0 version presented deficiencies, which have been solved in the latest TRACE release (5.0 patch 2). It is important to point out that the subcooled break flow in the previous tests does not play an important role, and thus this problem was not identified earlier. Even though the problems with the subcooled choked flow were solved with patch 2, the methodology presented in this paper allowed a quick assessment of the new version, and different issues were detected; therefore, TRACE5.0 was used in this paper.

Acknowledgments

This work was partly funded by the Swiss Federal Nuclear Safety Inspectorate ENSI (Eidgenössisches Nuklearsicherheitsinspektorat), within the framework of the STARS project (http://stars.web.psi.ch/). The authors are as well grateful to the OECD/NEA ROSA-2 project participants: JAEA for experimental data and the Management Board of the OECD/NEA ROSA-2 project for providing the opportunity to publish the results.

References

[1] F. Reventós, L. Batet, C. Llopis, C. Pretel, M. Salvat, and I. Sol, "Advanced qualification process of ANAV NPP integral dynamic models for supporting plant operation and control," *Nuclear Engineering and Design*, vol. 237, no. 1, pp. 54–63, 2007.

[2] C. Llopis, F. Reventós, L. Batet, C. Pretel, and I. Sol, "Analysis of low load transients for the Vandellòs-II NPP. Application to operation and control support," *Nuclear Engineering and Design*, vol. 237, no. 18, pp. 2014–2023, 2007.

[3] Paul Scherrer Institut, "Steady-state and transient analysis research of the swiss reactors (STARS project)," 2011, http://stars.web.psi.ch/.

[4] G. B. Treybal, *One-Dimensional Two-Phase Flow*, McGraw-Hill, New York, NY, USA, 1969.

[5] NEA-CSNI. Bemuse Phase V Report, "Uncertainty and sensitivity analysis of a LB-LOCA in ZION nuclear power plant," Tech. Rep., Committee on the Safety of Nuclear Installations, OECD, Nuclear Energy Agency, 2011.

[6] T. Yonomoto, "CCFL characteristics of PWR steam generator U-tubes," in *Proceedings of the ANS International Topic Meeting on Safety of Thermal Reactors*, Portland, Ore, USA, 2001.

[7] T. Takeda, M. Suzuki, H. Asaka, and H. Nakamura, "Quick-look data report of OECD/NEA ROSA project test 6-1 (1.9% pressure vessel upper-head small break LOCA experiment)," Tech. Rep. JAEA-Research 2006–9001, Japan Atomic Energy Agency, 2006.

[8] J. Freixa and A. Manera, "Analysis of an RPV upper head SBLOCA at the ROSA facility using TRACE," *Nuclear Engineering and Design*, vol. 240, no. 7, pp. 1779–1788, 2010.

[9] T. Takeda, M. Suzuki, H. Asaka, and H. Nakamura, "Quick-look data report of OECD/NEA ROSA project test 6-2 (0.1% pressure vessel bottom small break LOCA experiment)," Tech. Rep. JAEA-Research 2006–9002, Japan Atomic Energy Agency, 2006.

[10] T. Takeda, M. Suzuki, H. Asaka, and H. Nakamura, "Quick-look data report of test 1, test for hot leg intermediate break loss of coolant accident with break size equivalent to 17Flow area," Tech. Rep. JAEA-Research 2010-, Japan Atomic Energy Agency, 2010.

[11] J. Freixa, T.-W. Kim, and A. Manera, "Thermal-hydraulic analysis of an intermediate LOCA test at the ROSA facility including uncertainty evaluation," in *Proceedings of the 8th International Topical Meeting on Nuclear Thermal-Hydraulics, Operation and Safety (NUTHOS '10)*, Shanghai, China, October 2010.

[12] The ROSA-V Group, "ROSA-V large scale test facility (LSTF) system description for the third and fourth simulated fuel assemblies," Tech. Rep. JAERI-Tech 2003-037, Japan Atomic Energy Agency, 2003.

[13] T. Takeda, M. Suzuki, H. Asaka, and H. Nakamura, "Quick-look data report of ROSA-2/LSTF Test 2 (cold leg intermediate break LOCA IB-CL-03 in JAEA," Tech. Rep. JAEA-Research 2010-, Japan Atomic Energy Agency, 2010.

[14] T. Takeda, M. Suzuki, H. Asaka, and H. Nakamura, "Final data report of ROSA/LSTF Test 5-2 (primary cooling through

steam generator secondary-side depressurization experiment SB-CL-40 in JAEA)," Tech. Rep. JAEA-Research 2009-, Japan Atomic Energy Agency, 2009.

[15] H. Austregesilo and H. Glaeser, "Results of post-test calculation of LSTF Test 6-1 (SB-PV-09) with the code ATHLET," in *OECD/NEA ROSA Project, 4th PRG Meeting*, Tokai-mura, Japan, 2006.

[16] J. Freixa, "Post-test thermal-hydraulic analysis of ROSA Test 6.1," Tech. Rep. TM-41-08-10, Paul Scherrer Institut, 2008.

[17] H. Glaeser, "GRS analysis for CSNI uncertainty methods study (UMS)," Tech. Rep., Committee on the Safety of Nuclear Installations, OECD, Nuclear Energy Agency, 2011.

[18] E. Hofer and M. Kloos, *Relap5/Mod3.3 Code Manual. Volume I: Code Structure, System Models, and Solution Methods*, 2003.